RAA 2020 Vol. **20** No. **11**, 183(10pp) doi: 10.1088/1674-4527/20/11/183

http://www.raa-journal.org *http://iopscience.iop.org/raa*

Research in Astronomy and Astrophysics

Estimating up-limits of eccentricities for the binary black holes in the LIGO-Virgo catalog GWTC-1

Qian-Yun Yun[1,2], Wen-Biao Han[1,3], Gang Wang[1,3] and Shu-Cheng Yang[1,3]

[1] Shanghai Astronomical Observatory, Chinese Academy of Sciences, Shanghai 200030, China; *yqy@shao.ac.cn, wbhan@shao.ac.cn, gwang@shao.ac.cn*
[2] School of Physical Science and Technology, ShanghaiTech University, Shanghai 201210, China
[3] School of Astronomy and Space Science, University of Chinese Academy of Sciences, Beijing 100049, China

Received 2020 April 1; accepted 2020 May 24

Abstract In the first Gravitational-Wave Transient Catalogue of LIGO and Virgo, all events are announced having zero eccentricity. In the present paper, we investigate the performance of SEOBNRE, which is a spin-aligned eccentric waveform model in time-domain. By comparing with all the eccentric waveforms in SXS library, we find that the SEOBNRE coincides perfectly with numerical relativity data. Employing the SEOBNRE, we re-estimate the eccentricities of all black hole merger events. We find that most of these events allow a possibility for existence of initial eccentricities at 10 Hz band, but are totally circularized at the observed frequency ($\gtrsim$ 20 Hz). The upcoming update of LIGO and the next generation detector like Einstein Telescope will observe the gravitational waves starting at 10 Hz or even lower. If the eccentricity exists at the lower frequency, then it may significantly support the dynamical formation mechanism taking place in globular clusters.

Key words: gravitational waves — stars: black holes — binaries: general

1 INTRODUCTION

The successful detection of gravitational waves (GWs) by Advanced LIGO and Virgo (Abbott et al. 2016e,b,c,d,a, 2017a,b, 2019b,d,a) announces that the era of GW Astronomy is coming. Along with the more and more events will be found in the future, the formation mechanics and distribution of GW events might be revealed. Up to now, the Advanced LIGO and Virgo has announced 11 gravitational wave events, most of them (10) are coalescences of binary black holes (Abbott et al. 2019b) in the first LIGO-Virgo catalog GWTC-1. In the third run of Advanced LIGO and Virgo in 2019, more binary black hole mergers are detected (Abbott et al. 2018), for example the recent detection GW190412 is an asymmetric binary black hole (Abbott et al. 2020). In astrophysics, how these binary compact objects form is still an open issue. Usually, there are two main channels: isolated binary evolution and dynamical formation. These two channels admit the binary merging due to gravitational radiation within the cosmological age.

The mechanism of formation of binaries does not directly encode into the GW signals. However, the imprint of the formation channels may be the eccentricity of the binary orbit. There are viable formation channels including isolated binary evolution (Bethe & Brown 1998; Belczynski et al. 2002, 2014, 2016; Spera et al. 2015) and dynamical encounters (Portegies Zwart & McMillan 1999; O'Leary et al. 2006; Sadowski et al. 2008; Downing et al. 2010, 2011). In addition to these two main channels, Antonini et al. (2017) summarized several channels, dynamical exchange interactions in the dense stellar core of globular clusters or young massive star clusters (Rodriguez et al. 2015; Haster et al. 2016; Chatterjee et al. 2017; Banerjee 2017) and the evolution of isolated triples in galactic field (Silsbee & Tremaine 2016). Due to the GW radiation, at the last stage of the merger, the orbit will be definitely circularized (Hinder et al. 2008). This is the reason why all events observed so far do not show evidence of non-zero eccentricity. In the earlier stage, for example for a black hole binary with the radiated GW frequency at 10 Hz , the eccentricity should be negligible if the merger comes from the isolated binary evolution (Peters 1964; Hinder et al. 2008). In the other case, if the merger originates from dynamical formation, the eccentricity could be in a wide range when radiated wave

of binary at 10 Hz, even can be close to unity (Zevin et al. 2017, 2019b,a; Rodriguez & Antonini 2018; Samsing 2018; Gondan & Kocsis 2019). These researches also predicted that about 5% of dynamically-formed binaries have $e \geq 0.1$ at 10 Hz (Samsing 2018; Rodriguez et al. 2018). Recently, Takátsy et al. (2019) claimed the ratio of eccentric binaries in the aLIGO band is 10% for binaries formed through the Kozai-Lidov mechanism, and could be as large as 90% for gravitational capture formation.

In the first and second runs of advanced LIGO and Virgo, the starting GW frequency observed is more than 20 Hz (Abbott et al. 2016c). However, with the constant updating of LIGO, and the future Einstein Telescope[1], we can observe the GWs at 10 Hz or even lower for coalescence of binary compacts. So, we expect that we will be able to find the eccentric orbit at the lower frequency band. After enough events accumulated, the distribution of two channels may be revealed.

Usually, the search of eccentric GW sources needs waveform templates. Now in the LALsuite Library[2] (Vallisneri et al. 2015), there are EccentricFD (Huerta et al. 2014; Tiwari et al. 2016), EccentricTD and TaylorF2e (Moore & Yunes 2019), together with ready-to-use eccentric model (Tiwari et al. 2019) which only cover the inspiraling part of binary merger. For binary black hole (BBH) mergers, highly accurate models for eccentric orbits with the full inspiral-merger-ringdown waveforms are needed. A few of models (Huerta et al. 2018; Cao & Han 2017; Hinderer & Babak 2017; Hinder et al. 2018; Ireland et al. 2019) have been developed for this target. One of these models, the SEOBNRE (Cao & Han 2017) including spin and eccentricity has a very good consistence with numerical relativity data.

Before Advanced LIGO detected its first event GW150914, Tiwari et al. (2016) proposed how to search the eccentric binary black holes. Abbott et al. (2019c) announced the search result for eccentric binary black hole mergers during Advanced LIGO and Advanced Virgo's first and second observing runs. No candidate events were observed. In the next year, Nitz et al. (2020) searched for eccentric binary neutron star mergers in the first and second observing runs of Advanced LIGO with matched filtering technology by using EccentricFD model, and also no candidates were reported. Lower et al. (2018) and Romero-Shaw et al. (2019) using SEOBNRE to search eccentricity in the first gravitational transient catalogue of LIGO and Virgo (Abbott et al. 2019b), they tried to perform Bayesian inference to measure the possible eccentricities while these events at 10 Hz. They believe that all the eccentricities should be zero even at the 10 Hz band.

[1] `http://www.et-gw.eu/`.
[2] `https://wiki.ligo.org/DASWG/LALSuite`.

However, due to the very high noise at the 10 Hz band (Harry et al. 2010; Abbott et al. 2016c; Martynov et al. 2016), the above inference may not exclude the possibility of eccentricity at this low frequency stage, as they said, their analysis just yields no strong evidence for non-zero eccentricity in GWTC-1 (Abbott et al. 2019d). In the present paper, we use the SEOBNRE which proposed by one of the authors to do a theoretical constrain of the eccentricities of GWTC-1 events (Abbott et al. 2019c). We find that due to the fast circularization of the orbits by gravitational radiation (Redmount & Rees 1989; Will & Wiseman 1996; Hinder et al. 2008). Though we observe zero eccentricity at $\gtrsim$ 20 Hz, a big range of eccentricity distribution at 10 Hz is still theoretically allowed.

This paper is organized as follows. In the next section, we briefly introduce the SEOBNRE waveform model and demonstrate its performance on the modeling of eccentric waveforms. In the third section, by using SEOBNRE, we generate eccentric waveforms at 10 Hz and do matched filtering with all BBH events announced in GWTC-1. Finally, discussion is addressed in the last section.

2 THE PERFORMANCE OF SEOBNRE

2.1 The SEOBNRE Model

To describe the binary black holes, we use following parameters. The masses of two black holes are m_1 and m_2, and we assume $m_1 \geq m_2$. The total mass is $M = m_1 + m_2$, and the mass ratio is $q \equiv m_1/m_2$. In our paper, q is always larger than 1. The symmetric mass ratio is $\eta = m_1 m_2/M^2$. The spin of the two black holes are $\boldsymbol{S_1}$ and $\boldsymbol{S_2}$. Using units $c = G = 1$ in this section, we define the dimensionless spin parameters

$$\chi_i = \boldsymbol{S_i}/m_i^2 \tag{1}$$

with $\chi_i \in [-1, 1]$. In the present paper, we only consider the spin aligning with the orbital angular momentum of the binary, i.e., z direction.

The core idea of effective-one-body (EOB) theory treats a real two-body system as an equivalent one-body problem. Buonanno & Damour (1999) first proposed the effective-one-body approach for solving the problem of relativistic binary. The EOB formalism is more accurate than post-Newtonian approximation in Taylor expansion (Buonanno & Damour 1999). The EOB theory can give the complete process of the merger of compact binary, including the inspiral, merge and ringdown. After that, Buonanno et al. (2007) built an effective-one-body numerical-relativity (EOBNR) waveform model, which combines the effective-one-body theory and numerical relativity data. The updated EOBNR

model is SEOBNR, which is extended to the spinning black holes (Barausse & Buonanno 2011; Taracchini et al. 2012). SEOBNR has been proven to be useful for quasi-circular orbit without procession (Lovelace et al. 2016). Cao & Han (2017) extended SEOBNR to SEOBNRE for elliptic binary black hole merger, and has been used in a lot of data analysis to research for eccentric sources (Cao & Han 2017; Abbott et al. 2019c; Ramos-Buades et al. 2019; Liu et al. 2019). In the present work, we also employ the SEOBNRE to calculate GW waveforms with orbital eccentricity and to analyze the LIGO-Virgo GW data.

The EOB formalism includes three independent but interacting parts: (1) a description of the conservation part of the dynamics process of the compact binary (the Hamiltonian); (2) the radiation-reaction force; (3) the asymptotic gravitational waveform emitted by the binary.

The following is the simple summary of the conservation part for SEOBNRE. In the Newtonian two-body problem, we can equivalently use a "test particle" with a reduced mass to orbit the "center mass" M (M is the total mass of the two bodies). The EOB theory extends the Newtonian idea to general relativity, that is, to find an equivalent external space-time metric of a binary. In the EOB approach, we reduce the conservative dynamics of two-body problem to a geodesic motion of an effective test particle in an effectively deformed Kerr spacetime.

The EOB Hamiltonian can be written as (Barausse & Buonanno 2011; Taracchini et al. 2012)

$$H = M\sqrt{1+2\eta\left(\frac{H_{\rm eff}}{M\eta}-1\right)}, \tag{2}$$

$$H_{\rm eff} = H_{\rm NS} + H_{\rm S} + H_{\rm SC}. \tag{3}$$

where the details of $H_{\rm NS}, H_{\rm S}$ and $H_{\rm SC}$ can be found in Cao & Han (2017).

We can write the motion equation based on the Hamiltonian,

$$\dot{\boldsymbol{r}} = \frac{\partial H}{\partial \vec{p}}, \tag{4}$$

$$\dot{\boldsymbol{p}} = -\frac{\partial H}{\partial \boldsymbol{r}}. \tag{5}$$

Now we introduce the gravitational wave part of the model, the SEOBNRE model provides expressions for the $2,2$ spin-weighted spherical-harmonic modes of the GW signal. The inspiral waveform are decomposed into a quasi-circular part and an eccentricity part. First, the quasi-circular part is

$$\begin{aligned} h^{(C)}_{\ell m} &= h^{(N,\epsilon)}_{\ell m}\hat{S}^{(\epsilon)}_{\rm eff}T_{\ell m}e^{i\delta_{\ell m}}\left(\rho_{\ell m}\right)^{\ell}N_{\ell m}{\rm with}h^{(N,\epsilon)}_{\ell m} \\ &= \frac{M\eta}{R}n^{(\epsilon)}_{\ell m}c_{\ell+\epsilon}V^{\ell}_{\Phi}Y^{\ell-\epsilon,-m}\left(\frac{\pi}{2},\Phi\right), \end{aligned} \tag{6}$$

where R is the distance between detector and source, Φ is the orbital phase, and $Y^{\ell m}(\Theta,\Phi)$ are the scalar spherical harmonics. Second, the $(2,2)$ mode containing eccentric part is

$$\begin{aligned} h_{22} = 2\eta\Big[&\Theta_{ij}\left(Q^{ij}+P_0Q^{ij}+P^{\frac{3}{2}}Q^{ij}_{\rm tail}\right) \\ &+P_n\Theta_{ij}\left(P^{\frac{1}{2}}_nQ^{ij}+P^{\frac{3}{2}}_nQ^{ij}\right) \\ &+P_v\Theta_{ij}\left(P^{\frac{1}{2}}_vQ^{ij}+P^{\frac{3}{2}}_vQ^{ij}\right) \\ &+P_{nn}\Theta_{ij}P_{nn}Q^{ij}+P_{nv}\Theta_{ij}P_{nv}Q^{ij} \\ &+P_{vv}\Theta_{ij}P_{vv}Q^{ij}+P_{nnv}\Theta_{ij}P^{\frac{3}{2}}_{nv}Q^{ij} \\ &+P_{nvv}\Theta_{ij}P^{3}_{vvv}Q^{ij}+P_{vvv}\Theta_{ij}P^{\frac{3}{2}}_{vvv}Q^{ij}\Big]. \end{aligned}$$

All the coefficients listed in the above equations can be found in Cao & Han (2017).

2.2 Validation of Elliptic Waveforms with Numerical Relativity Data

In this subsection, we compare the SEOBNRE waveforms with NR data to validate this theoretical waveform model, because description of a binary black hole by SEOBNRE depends on several approximations while the NR waveform is the direct solution to the Einstein equation. It is a standard procedure that using the numerical-relativity (NR) waveform to validate an approximated waveform (Baumgarte & Shapiro 2010). The NR data that we used are downloaded from *https://www.black-holes.org/code/SpEC.html* (Mroue et al. 2013; Blackman et al. 2015; Boyle et al. 2019). The quantitatively comparison between the approximate waveforms (h_1) and the numerical-relativity waveforms (h_2) is using the standard inner product weighted by $S_n(f)$ (the power spectral density of the detector noise, here we use the LIGO's sensitivity curve).

The SEOBNRE can generate the complete waveform including inspiral, merge and ringdown. The waveform of binary coalescence has an amplitude peak, usually this moment is labeled as $t = 0$. We align the NR and SEOBNRE waveforms at the amplitude peak to do the comparison. The inner product is defined as (Cutler & Flanagan 1994),

$$\langle h_1, h_2\rangle = 4\,{\rm Re}\int_{f_{\rm min}}^{f_{\rm max}}\frac{\tilde{h}_1(f)\tilde{h}^*_2(f)}{S_n(f)}df\,. \tag{7}$$

The normalized match can be optimized over a relative time shift and the initial orbital phase; i.e., the fitting factor of two signals is,

$${\rm FF} = \max\left[\frac{\langle h_1|h_2\rangle}{\sqrt{\langle h_1|h_1\rangle\,\langle h_2|h_2\rangle}}\right], \tag{8}$$

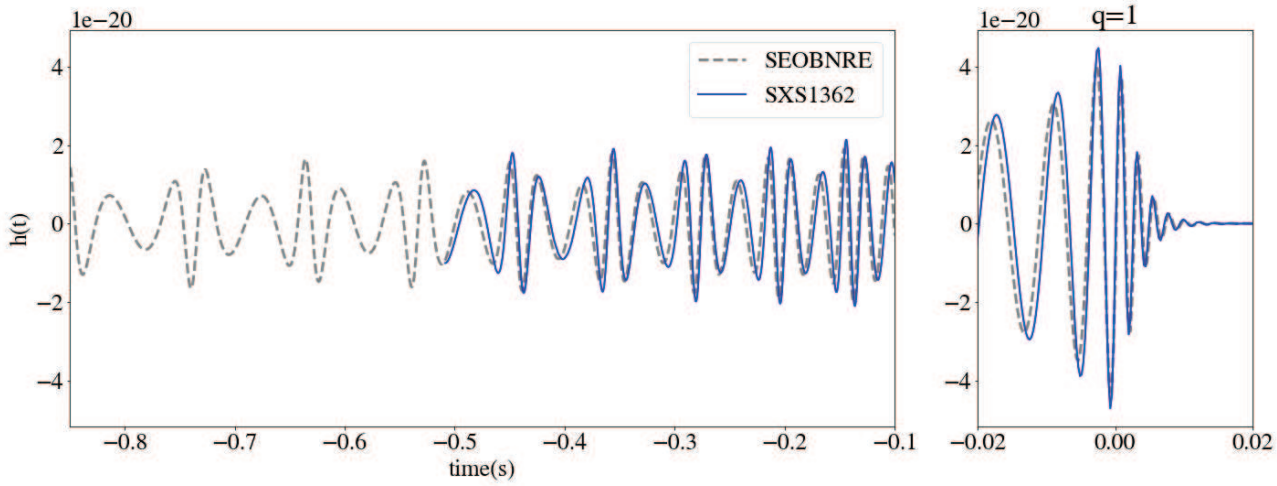

Fig. 1 NR (BBH:SXS1362) and SEOBNRE waveforms for equal-mass spinless BH binary with $m_1 = m_2 = 20m_\odot$. The initial eccentricity of SXS1362 is $e < 1.7$, and the one of SEOBNRE waveform is 0.401 at 20 Hz. The match between the two waveforms is 0.9905.

and the mismatch of two signals is defined as 1-FF. For a given NR waveform, we set the parameters like total mass M, mass ratio q and the individual spin $\chi_{1,2}$. We evaluate the SEOBNRE waveform between a frequency range of 20 and 2000 Hz. When we calculate the theoretical waveforms, we use the same M, q, χ of the NR waveform, but do not use the NR eccentricity to set the eccentricity in SEOBNRE. Because the eccentricity changes with GW's (or orbital) frequency and the orbit is not closed ellipse, the eccentricity in NR waveform may not be extracted precisely.

In Figure 1, we plot both the SEOBNRE and NR waveforms for an equal-mass spinless BBH case (BBH:1362 in SXS data, $m_1 = m_2 = 20m_\odot$) without spin. By setting the initial eccentricity of SEOBNRE equals 0.401 at 20 Hz, we get the best coincidence of two waveforms, and the match of them is 0.9905.

Figure 2 shows the match results of a few NR waveforms with SEOBNRE ones for equal mass and nonspinning binaries. The match results keep good with the increasing of the eccentricity. Most of matches are better than 99% even for the large eccentricity. However, the mismatch still slightly increases when the eccentricity grows larger. This is clearly shown in the figure.

Now we investigate the performance of SEOBNRE for general BBHs with spins or varied mass-ratios. For this target, we use 14 NR BBH waveforms (SXS:320-324, SXS:1364-1373). Among them, SXS:320-324 are spin-aligned BBHs, with $\chi_1 = 0.44$, $\chi_2 = -0.33$, and the mass ratio $q = 1.22$. The eccentricities of these BBHs are in a range [0, 0.3]. SXS:1364-1373 are nonspinning binaries but the mass ratio is 2:1 or 3:1. In Table 1, we list the match results of NR data with SEOBNRE waveforms

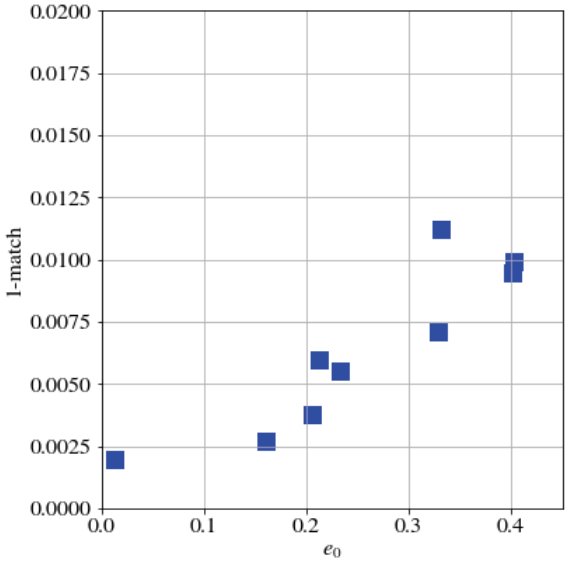

Fig. 2 The mismatch between the NR waveforms and SEOBNRE waveforms for equal-mass and nonspinning binaries, e_0 represents the initial eccentricity of the SEOBNRE waveform when the GW frequency is 20 Hz as assuming $m_1 = m_2 = 20m_\odot$.

in the third column. One can see that all the matches are larger than 0.98. Considering a standard criterion of 97% in fitting factor, together with the results in Figures 2 and 4, we have enough confidence for the SEOBNRE template in the cases of spinning and unequal mass-ratio BBHs with eccentricities. In addition, we also compare the eccentricities in the NR data and the ones in the SEOBNRE model.

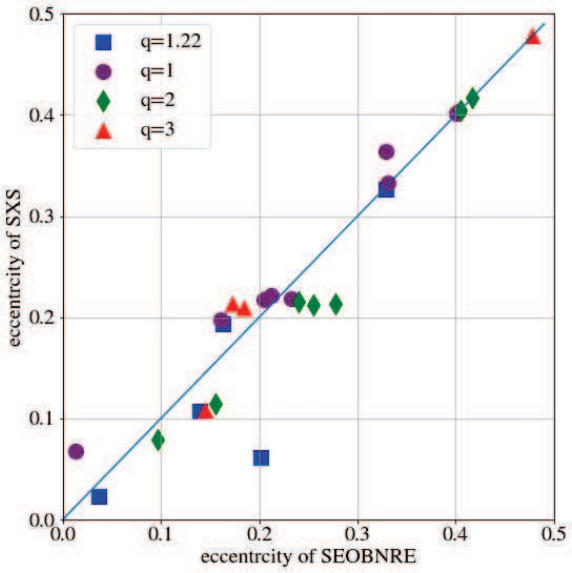

Fig. 3 Comparison the eccentricity of SEOBNRE at 20 Hz and the eccentricity given by the NR waveform, using different color to distinct different mass ratio, the mass ratio is indicated on the label, the eccentricity of SEOBNRE is all bigger when the mass ratio is 2 and 3. when mass ratio $q = 1$, the eccentricity of SEOBNRE is a little smaller than the NR's eccentricity.

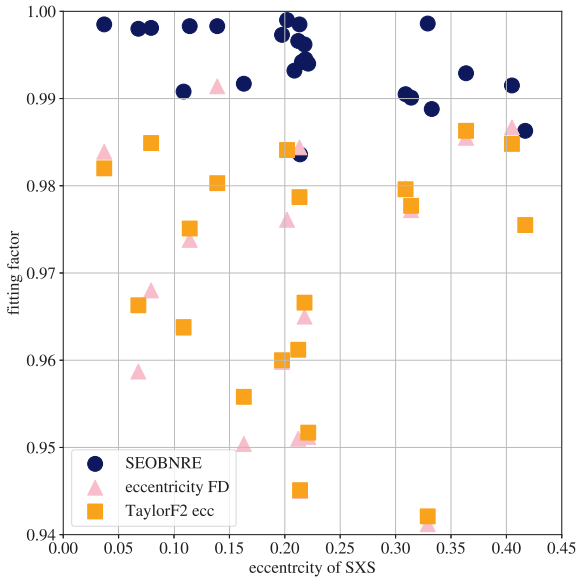

Fig. 4 Match results between SXS numerical relativity data with the SEOBNRE waveforms, EccentricFD and TalorF2 ecc templates.

We also compare the eccentricities defined in NR waveforms and SEOBNRE ones. Most of the eccentricities coincide each other in an acceptable error, see Figure 3 for details. We notice that the initial eccentricities of SEOBNRE waveforms are usually larger than the ones in NR data when the mass-ratio is 1.22 and 2. However, when mass ratio equals one, the eccentricities of SEOBNRE waveforms are slightly smaller than the NR ones. One possible reason for these differences is the different initial frequency between our waveforms and SXS ones. When we generate the SEOBNRE waveforms, we must ensure our waveforms are slightly longer than SXS ones, because we need to cut our waveforms to align with the SXS ones for comparison. At the inspiral stage of a BBH, the eccentricity of the orbit changes with the frequency. For some NR cases without physical eccentricities (such as 324, 1362 etc.), SEOBNRE can offer reference values.

There are several gravitational wave templates containing orbital eccentricity which have been implemented in LIGO Libraries and LALSuite, such as EccentricFD and TaylorF2 ecc, which are non-spinning frequency domain waveform templates for elliptic binaries Tanay et al. (2016); Huerta et al. (2014). They both only describe the inspiraling part of the gravitational waves without the merger and ringdown waveforms. Considering the EccentricFD and TalorF2 ecc models are inspiral-only templates, so there is a sharp cutoff in the end of the waveform. For matching with NR data, we need cut the NR waveforms to keep only the inspiral part.

The match results of these two templates are also shown in Figure 4, which shows all the matches of three templates with NR data. From these results, we can see that the SEOBNRE performs much better than the other two templates when the BBHs having spins, asymmetric mass-ratio and nonzero eccentricities. After that, we also calculated the match between SXS and EccentricTD which is a time domain waveform with orbital eccentricity in LALsuite. Table 1 lists all the information about the BBH number of the SXS, the eccentricity of SXS, the match between SEOBNRE waveforms and SXS ones, the eccentricity of SEOBNRE at 20 Hz, the match between EccentricFD and SXS data, the match between EccentricTD and SXS data, the match between TaylorF2 ecc and SXS data. In Table 1, most SEOBNRE waveform exhibits mismatches of typically less than 1%.

Because the EccentricFD and TaylorF2 ecc waveforms are shorter than the complete waveforms, then the signal-to-noises (SNRs) will be smaller than the SEOBNRE model. We calculate their optimal SNR and compare to the SEOBNRE one as follows:

$$\mathrm{SNR}^2 = 4\,\mathrm{Re}\int_{f_{\min}}^{f_{\max}} \frac{\tilde{h}_1(f)\tilde{h}_1^*(f)}{S_n(f)} df\,. \tag{9}$$

Considering that SEOBNRE is a time-domain model, we do the FFT before we calculate the SNR, transferring the time-domain waveform to a frequency-domain one. We

Table 1 Match results between SXS numerical relativity data with the SEOBNRE waveforms, EccentricFD , EccentricTD and TalorF2 ecc templates.

SXS number	SXS ecc.	SEOBNRE match	SEOBNRE ecc.	eccFD match	eccTD match	TaylorF2 match
320	0.0227	0.9985	0.037	0.9839	0.9403	0.9820
321	0.0611	0.999	0.202	0.9761	0.9466	0.9841
322	0.1070	0.9983	0.139	0.9914	0.9319	0.9803
323	0.1936	0.9917	0.163	0.9504	0.9235	0.9558
324	NaN	0.9986	0.329	0.9412	0.8034	0.9421
1355	0.0678	0.998	0.013	0.9587	0.9371	0.9663
1356	0.1974	0.9973	0.161	0.9598	0.9550	0.9600
1357	0.2211	0.9940	0.212	0.9512	0.9248	0.9517
1358	0.2186	0.9945	0.233	0.9379	0.9194	0.9384
1359	0.2177	0.9962	0.205	0.9650	0.9246	0.9666
1360	0.3635	0.9929	0.241	0.9855	0.8899	0.9863
1361	0.3326	0.9888	0.212	0.8882	0.8415	0.8884
1362	< 1.7	0.9905	0.309	0.9797	0.8280	0.9796
1363	< 1.8	0.9901	0.314	0.9772	0.8644	0.9777
1364	0.0793	0.9981	0.097	0.9680	0.9343	0.9849
1365	0.1141	0.9983	0.155	0.9738	0.9273	0.9751
1366	0.2154	0.9942	0.24	0.9230	0.8992	0.9373
1367	0.2132	0.9985	0.277	0.9844	0.8909	0.9787
1368	0.2121	0.9966	0.255	0.9510	0.9230	0.9612
1369	< 1.8	0.9915	0.405	0.9867	0.7663	0.9848
1370	< 1.7	0.9863	0.417	0.9755	0.8772	0.9755
1371	0.1086	0.9908	0.145	0.9637	0.8930	0.9638
1372	0.2137	0.9836	0.173	0.9450	0.8775	0.9451
1373	0.2086	0.9932	0.184	0.9299	0.8720	0.9329

choose four eccentric binaries of different mass ratio from all SXS waveforms in the present work. The SNRs of four BBHs are shown in Table 2, we can see the inspiral-merge-ringdown waveforms calculated by SEOBNRE have higher SNRs than the inspiral only waveforms (EccentricFD and TalorF2 ecc). This suggests that we should use SEOBNRE to find the potential eccentric GWs in LIGO-Virgo data, if the efficiency of SEOBNRE has been improved. For calculation, we take the total mass (M) as 40 solar mass, and the luminosity distance from the detector to the GW source as 100 Mpc.

The comparison of SEOBNRE with NR has been discussed comprehensively by Liu et al. (2019). Here we get the same result that the SEOBNRE performs perfectly for eccentric binaries. In addition, we compare the two templates (EccFD and Taylor F2e) in LALSuite with SEOBNRE. The performance of these PN models are worse than the SEOBNRE and they will induce a loss of about 30% SNRs.

3 ESTIMATING ECCENTRICITIES AT EARLIER STAGE OF LIGO EVENTS

As we have mentioned before, all the gravitational wave sources in GWTC-1 have no eccentricity. This is because maybe all the events come from isolated evolution, and the eccentricity can be ignored before merger. However, maybe some of them have wild eccentricities at the earlier stage, and loss eccentricities due to the rapid circularizing at the final inspiraling stage when enter the LIGO's sensitive band. The circularization and the merger time scale can be estimated by Peters through post-Newtonian approximation in (Peters 1964)

$$\frac{de}{dt} = -\frac{304}{15}\frac{M^3\eta}{a^4\left(1-e^2\right)^{5/2}}e\left(1+\frac{121}{304}e^2\right) , \quad (10)$$

$$T = \frac{768}{425}\frac{5a^4}{256M^3\eta}\left(1-e^2\right)^{7/2} , \quad (11)$$

where a is the semi-major of an orbit.

As we mentioned, a few of models predict that the eccentricity could be in a wide range when the radiated wave of binary at 10 Hz if the BBHs originate from dynamical formation. From the above equations, the eccentricity will be reduced to zero when GWs enter the detectable frequency (> 20 Hz) of the first LIGO run.

For investigating this possibility, we employ the SEOBNRE model and the binary black holes events released in the LIGO-Virgo catalog GWTC-1. Firstly, using the SEOBNRE, elliptic waveforms starting from 10 Hz are generated with the same parameters of the public BBH events. Secondly, consider the sensitivity in the first run of LIGO, we only use the LIGO data of each event starting from 20 Hz. Therefore, the SEOBNRE waveforms are used for data analysis also from 20 Hz, though the waveforms are calculated from 10 Hz with initial eccentricity. Finally, we match the theoretical waveforms and observed signals, calculate the matched-filtering SNR. The PSD of detector for each event is estimated by using the neighboring data (16 seconds before and 16 seconds after the event).

Table 2 The optimal matched filtering SNRs by using different waveforms, with NR data as "real" signals. The PN templates lose SNR due to shorter signals.

mass ratio	SEOBNRE optimal SNR	eccFD optimal SNR	Taylor F2e optimal SNR
1.00	35.6	24.5	24. 5
1.22	30.0	23.8	23. 8
2.00	37.0	21.6	23. 4
3.00	29.4	21.4	21. 4

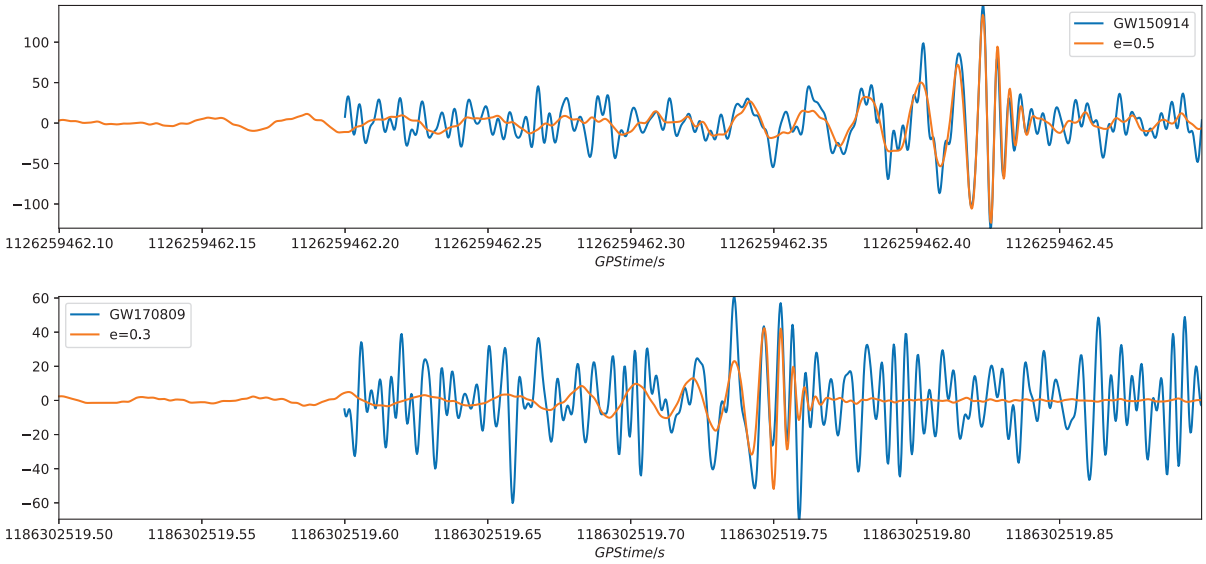

Fig. 5 *Top panel*: The SEOBNRE waveforms with $e_0 = 0.5$ at 10 Hz and GW150914 signals; *Bottom panel*: The SEOBNRE waveforms with $e_0 = 0.3$ at 10 Hz and GW170809 signals.

In Figure 5, as examples, we demonstrate two SEOBNRE waveforms (noise added) together with the LIGO's signals GW150914 and GW 170809. With initial eccentricities of 0.5 and 0.3 at 10 Hz respectively, the SEOBNRE waveforms coincide with the two signals observed by the LIGO Hanford Observatory. This means that there is a possibility that these two BBHs allow eccentricities up to 0.5 and 0.3 at 10 Hz.

After investigating all the ten BBH data, we find seven of them cannot rule out possible eccentricities at 10 Hz. The matched-filtering SNRs with SEOBNRE templates of these seven events are larger than or equal the SNRs announced in LIGO-Virgo catalog. All of the data analysis are done by the software in LALsuite Library. In Table 3, we list the results of all these seven events.The second column lists the maximal allowed eccentricities in these events with the same SNRs of LIGO released.

In Figure 6, the variation of SNRs of four events (GW150914, GW170104, GW170809 and GW170814) with initial eccentricities at 10 Hz is plotted. One can see that the SNRs drop suddenly if the initial eccentricities in the SEOBNRE waveforms exceed some critical values. We then assume that these events allow the possibility of orbital eccentricities at the 10 Hz stage. It is possible that all these events are still circular orbits at this earlier stage.

From the above analysis, the possible range of initial eccentricities at 10 Hz of these seven BBH events is $[0,\ e_{\max}]$. Our results only can declare that the current analysis cannot rule out the possibility of ecliptic orbits at 10 Hz band. The initial frequency of the SEOBNRE waveforms with eccentricity is 10 Hz, so all the initial eccentricity we talk about in this section is the eccentricity at 10 Hz.

We must emphasize that the $e_{\max}$ listed in Table 3 are not the measurement or estimation of the eccentricity of BBHs, just are the maximal allowed values at 10 Hz. It is still very possible that the eccentricity at 10 Hz is zero. The estimation of eccentricity of the binary black hole merger events in the first catalogue of LIGO and Virgo has been done by Romero-Shaw et al. (2019). They employed Bayesian inference to measure the eccentricity, and their analysis yields no strong evidence for non-zero eccentricity in the ten BBH events. However, we do not think that our result is conflicted with the one of Romero-Shaw et al. (2019). Our result is more like a theoretical constraint on the eccentricity at lower frequency band, due to the noise of LIGO's O1 and O2.

Table 3 The matched-filtering SNRs by using SEOBNRE templates of seven detected BBH events and possible maximum eccentricities at 10 Hz.

Events	possible $e_{\max}$ at 10 Hz	SNR	$m_1(M_\odot)$	$m_2(M_\odot)$	effective inspiral spin
GW150914	0.5	26.42	35.6	30.6	−0.01
GW170814	0.08	17.6	30.6	25.2	0.08
GW170104	0.08	13.3	30.8	20.0	−0.04
GW170809	0.32	12.69	35.0	23.8	0.08
GW170823	0.26	11.38	39.5	29.0	0.09
GW170729	0.26	10.42	50.2	34.0	0.37
GW170818	0.35	10.47	35.4	26.7	−0.09

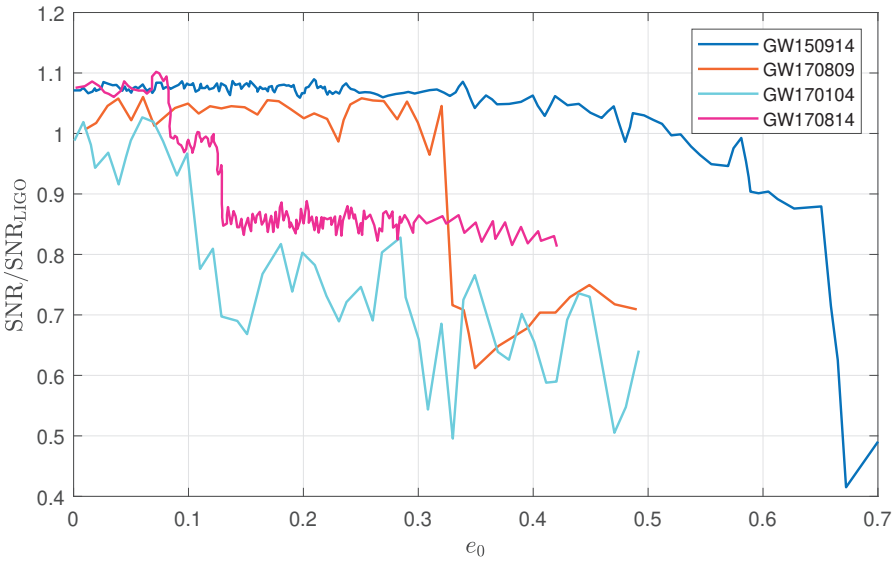

Fig. 6 Variation of the matched-filtering SNRs with initial eccentricities for four BBH events. The vertical axis represents the ratio between the matched-filtering SNR and the LIGO official one.

However, as a consequence of using only a point-estimate through matched filtering instead of the 90% confidence interval of a posterior probability distribution, our results are weaker bounds on eccentricity than the full Bayesian analysis by Romero-Shaw et al. (2019).

4 CONCLUSIONS

The formation mechanism of binary black hole mergers is an attractive topic in astrophysics, and eccentricity of binary is a useful clue to distinguish the origin of BBHs. Up to now, all LIGO-Virgo BBH events are announced as circular binaries. However, due to the poor sensitivity relatively in the first run of LIGO, this declaration may be only completely correct for these GW events when they enter $\gtrsim$ 20 Hz band; i.e., the final inspiral stage.

In the present paper, by employing SEOBNRE, a full waveform templates including inspiral, merger and ringdown phases, we try to investigate the possibility that these BBH events may originate from ecliptic binaries when the GWs that they radiated are at 10 Hz band. The choice of 10 Hz is based on two reasons. One is that the Advanced LIGO is improving its sensitivity after 10 Hz band, and maybe the data from this frequency will be available in the future. The other one is that some theoretical predictions show a few friction of dynamically-formed binaries having nonzero eccentricity at 10 Hz.

By comparing with numerical relativity data, we validate that SEOBNRE is a reliable waveform model for elliptic binaries, and have better performance than the frequency-domain templates in LALsuite Library. We then use SEOBNRE to generate theoretical gravitational waveforms from 10 Hz with eccentricity from 0 to 0.7. With the matched-filtering technology, we analyze the LIGO data of ten BBH events in the first catalog GWTC-1, and find that elliptic waveforms with initial eccentricities at 10 Hz can match very good with the observed signals after 20 Hz for seven BBH events.

Therefore, we conjecture that all these seven events still allow to exist eccentricities at the earlier stage (10 Hz band). However, it must be emphasized that we do not measure the eccentricities at 10 Hz, and we do not announce that these events are elliptic at this frequency band. Our results simply show that nonzero eccentricities at 10 Hz of these events are possible. Due to the orbital

circularization by gravitational radiation, the eccentricity reduces to zero after the GW frequency goes into 20 Hz.

In the near future, along with the update of Advanced LIGO and Virgo, GW data from 10 Hz will be available. The launch of multi-band gravitational wave observation with space-based detectors will enable us to study low-frequency ($10^{-4} \sim 1$ Hz) GWs. More information about a target binary will be acquired from the observed data. One can then really measure the eccentricities of binary mergers at this frequency band. The detection of an eccentric binary can not only prove that the binary can form dynamically but also distinguish the different dynamical formation (dynamical encounter or Kozai-Lidov oscillations in triple systems).

Acknowledgements This work is support by the National Natural Science Foundation of China (Grant Nos. 11273045 and 11773059) and by Key Research Program of Frontier Sciences, Chinese Academy of Sciences (No. QYZDB-SSW-SYS016). We also appreciate the useful discussions with Prof. Zhoujian Cao and Xiao-Lin Liu. This work was also supported by MEXT, JSPS Leading-edge Research Infrastructure Program, JSPS Grant-in-Aid for Specially Promoted Research 26000005, JSPS Grant-in-Aid for Scientific Research on Innovative Areas 2905: JP17H06358, JP17H06361 and JP17H06364, JSPS Core-to-Core Program A. Advanced Research Networks, JSPS Grant-in-Aid for Scientific Research (S) 17H06133, the joint research program of the Institute for Cosmic Ray Research, University of Tokyo.

References

Abbott, B. P., Abbott, R., Abbott, T., et al. 2016a, ApJL, 818, L22
Abbott, B. P., Abbott, R., Abbott, T., et al. 2016b, Physical Review X, 6, 041015
Abbott, B. P., Abbott, R., Abbott, T., et al. 2016c, Classical and Quantum Gravity, 33, 134001
Abbott, B. P., Abbott, R., Abbott, T., et al. 2016d, Physical Review Letters, 116, 241103
Abbott, B. P., Abbott, R., Abbott, T., et al. 2016e, arXiv preprint arXiv:1602.03841
Abbott, B. P., Abbott, R., Abbott, T., et al. 2017a, Classical and Quantum Gravity, 34, 044001
Abbott, B. P., Abbott, R., Abbott, T., et al. 2017b, ApJL, 851, L35
Abbott, B. P., Abbott, R., Abbott, T., et al. 2018, Living Reviews in Relativity, 21, 3
Abbott, B., Abbott, R., Abbott, T., et al. 2019a, ApJL, 882, L24
Abbott, B., Abbott, R., Abbott, T., et al. 2019b, Physical Review X, 9, 031040
Abbott, B., Abbott, R., Abbott, T., et al. 2019c, ApJ, 883, 149
Abbott, B., Abbott, R., Abbott, T., et al. 2019d, Physical Review Letters, 123, 011102
Abbott, R., et al. 2020, arXiv:2004.08342
Antonini, F., Toonen, S., & Hamers, A. S. 2017, ApJ, 841, 77
Banerjee, S. 2017, MNRAS, 467, 524
Barausse, E., & Buonanno, A. 2011, Physical Review D, 84, 104027
Baumgarte, T. W., & Shapiro, S. L. 2010, Numerical Relativity: Solving Einstein's Equations on the Computer (Cambridge Univ. Press)
Belczynski, K., Buonanno, A., Cantiello, M., et al. 2014, ApJ, 789, 120
Belczynski, K., Holz, D. E., Bulik, T., & O'Shaughnessy, R. 2016, Nature, 534, 512
Belczynski, K., Kalogera, V., & Bulik, T. 2002, ApJ, 572, 407
Bethe, H. A., & Brown, G. 1998, ApJ, 506, 780
Blackman, J., Field, S. E., Galley, C. R., et al. 2015, Physical Review Letters, 115, 121102
Boyle, M., Hemberger, D., Iozzo, D. A., et al. 2019, Classical and Quantum Gravity, 36, 195006
Buonanno, A., & Damour, T. 1999, Physical Review D, 59, 084006
Buonanno, A., Pan, Y., Baker, J., et al. 2007, Physical Review D, 76, 104049
Cao, Z., & Han, W.-B. 2017, Physical Review D, 96, 044028
Chatterjee, S., Rodriguez, C. L., Kalogera, V., & Rasio, F. A. 2017, The Astrophysical Journal Letters, 836, L26
Cutler, C., & Flanagan, E. E. 1994, Physical Review D, 49, 2658
Downing, J., Benacquista, M., Giersz, M., & Spurzem, R. 2010, MNRAS, 407, 1946
Downing, J., Benacquista, M., Giersz, M., & Spurzem, R. 2011, MNRAS, 416, 133
Gondan, L., & Kocsis, B. 2019, ApJ, 871, 178
Harry, G. M., Collaboration, L. S., et al. 2010, Classical and Quantum Gravity, 27, 084006
Haster, C.-J., Antonini, F., Kalogera, V., & Mandel, I. 2016, ApJ, 832, 192
Hinder, I., Kidder, L. E., & Pfeiffer, H. P. 2018, Physical Review D, 98, 044015
Hinder, I., Vaishnav, B., Herrmann, F., Shoemaker, D. M., & Laguna, P. 2008, Physical Review D, 77, 081502
Hinderer, T., & Babak, S. 2017, Physical Review D, 96, 104048
Huerta, E., Kumar, P., McWilliams, S. T., O'Shaughnessy, R., & Yunes, N. 2014, Physical Review D, 90, 084016
Huerta, E., Moore, C., Kumar, P., et al. 2018, Physical Review D, 97, 024031
Ireland, B., Birnholtz, O., Nakano, H., West, E., & Campanelli, M. 2019, Physical Review D, 100, 024015
Liu, X., Cao, Z., & Shao, L. 2019, arXiv preprint arXiv:1910.00784
Lovelace, G., Lousto, C. O., Healy, J., et al. 2016, Classical and Quantum Gravity, 33, 244002

Lower, M. E., Thrane, E., Lasky, P. D., & Smith, R. 2018, Physical Review D, 98, 083028
Martynov, D. V., Hall, E., Abbott, B., et al. 2016, Physical Review D, 93, 112004
Moore, B., & Yunes, N. 2019, Classical and Quantum Gravity, 36, 185003
Mroue, A. H., Scheel, M. A., Szilagyi, B., et al. 2013, Physical Review Letters, 111, 241104
Nitz, A. H., Lenon, A., & Brown, D. A. 2020, ApJ, 890, 1
O'Leary, R. M., Rasio, F. A., Fregeau, J. M., Ivanova, N., & O'Shaughnessy, R. 2006, ApJ, 637, 937
Peters, P. C. 1964, Physical Review, 136, B1224
Ramos-Buades, A., Husa, S., Pratten, G., et al. 2019, arXiv preprint arXiv:1909.11011
Redmount, I., & Rees, M. 1989, Comments on Astrophysics, 14, 165
Rodriguez, C. L., Amaro-Seoane, P., Chatterjee, S., & Rasio, F. A. 2018, Physical Review Letters, 120, 151101
Rodriguez, C. L., & Antonini, F. 2018, ApJ, 863, 7
Rodriguez, C. L., Morscher, M., Pattabiraman, B., et al. 2015, Physical Review Letters, 115, 051101
Romero-Shaw, I. M., Lasky, P. D., & Thrane, E. 2019, MNRAS, 490, 5210
Sadowski, A., Belczynski, K., Bulik, T., et al. 2008, ApJ, 676, 1162
Samsing, J. 2018, Physical Review D, 97, 103014
Silsbee, K., & Tremaine, S. 2016, arXiv preprint arXiv:1608.07642
Spera, M., Mapelli, M., & Bressan, A. 2015, MNRAS, 451, 4086
Takátsy, J., Bécsy, B., & Raffai, P. 2019, MNRAS, 486, 570
Tanay, S., Haney, M., & Gopakumar, A. 2016, Physical Review D, 93, 064031
Taracchini, A., Pan, Y., Buonanno, A., et al. 2012, Physical Review D, 86, 024011
Tiwari, S., Gopakumar, A., Haney, M., & Hemantakumar, P. 2019, Physical Review D, 99, 124008
Tiwari, V., Klimenko, S., Christensen, N., et al. 2016, Physical Review D, 93, 043007
Vallisneri, M., Kanner, J., Williams, R., Weinstein, A., & Stephens, B. 2015, in Journal of Physics: Conference Series, 610, 012021
Will, C. M., & Wiseman, A. G. 1996, Physical Review D, 54, 4813
Zevin, M., Kremer, K., Siegel, D. M., et al. 2019a, ApJ, 886, 4
Zevin, M., Pankow, C., Rodriguez, C. L., et al. 2017, ApJ, 846, 82
Zevin, M., Samsing, J., Rodriguez, C., Haster, C.-J., & Ramirez-Ruiz, E. 2019b, ApJ, 871, 91
Portegies Zwart, S. F., & McMillan, S. L. 2000, ApJL, 528, L17